Colony-forming and single-cell picocyanobacteria nitrogen acquisition strategies and carbon fixation in the brackish Baltic Sea

Christien P. Laber [1,2] Javier Alegria Zufia [1] Catherine Legrand [1,3] Elin Lindehoff [1]
Hanna Farnelid [1]*

[1]Department of Biology and Environmental Science, Centre for Ecology and Evolution in Microbial Model Systems (EEMiS), Linnaeus University, Kalmar, Sweden
[2]Department of Arctic and Marine Biology, UiT The Arctic University of Norway, Tromsø, Norway
[3]School of Business, Innovation and Sustainability, Halmstad University, Halmstad, Sweden

Abstract

Picocyanobacteria are widespread and globally significant primary producers. In brackish waters, picocyanobacterial populations are composed of diverse species with both single-cell and colony-forming lifestyles. Compared to their marine counterparts, brackish picocyanobacteria are less well characterized and the focus of research has been weighted toward single-cell picocyanobacteria. Here, we investigate the uptake dynamics of single and colony-forming picocyanobacteria using incubations with dual carbon-13 and inorganic (ammonium and nitrate) or organic (urea and amino acids) nitrogen-15 sources during August and September 2020 in the central Baltic Sea. Phytoplankton community and group-specific uptake rates were obtained using an elemental analyzer isotope ratio mass spectrometer (EA-IRMS) and nano secondary-ion mass spectrometry (NanoSIMS). Picocyanobacteria contributed greater than one third of the ammonium, urea, amino acids, and inorganic carbon community uptake/fixation in September but < 10% in August when phytoplankton biomass was higher. Overall, single-cell ammonium and urea uptake rates were significantly higher for single-celled compared to colonial picocyanobacteria. In a 6-yr offshore central Baltic Sea time series (2015–2020), summer abundances of colonial picocyanobacteria reached up to 10^5 cells mL^{-1} and represented > 5% of the average phytoplankton biomass, suggesting that they are periodically important for the ecosystem. Colonial strain identification was not distinguishable using 16S rRNA gene amplicon data, highlighting a need for refined tools for identification of colonial forms. This study shows the significance of single-celled brackish picocyanobacteria to nutrient cycling and the importance of considering uptake and lifestyle strategies when assessing the role of picocyanobacteria in aquatic ecosystems.

Picocyanobacteria are a diverse group of photosynthetic microorganisms that inhabit a broad range of marine, estuarine, brackish, and freshwater systems as well as extreme environments, with taxonomic and physiological diversity dependent on the environment of study (Callieri 2008; Maugeri et al. 2013; Farrant et al. 2016). In marine waters, picocyanobacterial

*Correspondence: hanna.farnelid@lnu.se

Additional Supporting Information may be found in the online version of this article.

assemblages are dominated by *Prochlorococcus* in oligotrophic central gyres and *Synechococcus* at higher altitudes and coastal regions (Flombaum et al. 2013). Meanwhile, freshwater systems exhibit a higher taxonomic diversity than marine systems, likely due to distinct geographic borders allowing more rapid speciation (Callieri et al. 2012). Brackish ecotypes can exhibit a mix of features found in both marine and freshwater relatives (Cabello-Yeves et al. 2022; Aguilera et al. 2023).

Assessing the diversity of picocyanobacteria remains an ongoing endeavor with lifestyle characteristics commonly misaligned with phylogenic placements. In freshwater, estuaries and brackish environments, many picocyanobacteria live in a variety of colony forms where colony size can range from tens to hundreds of cells (Callieri 2010). Colonies often form distinct morphologies driven by shape or orientation of cells within the colony, allowing for visual verification of species (e.g., *Aphanothece*, *Chroococcus*, and *Aphanocapsa*). However, the morphological identification of these genera has been under revision as molecular sequencing has separated

previously uniform genera such as *Aphanothece* into separate orders and genera that additionally include taxa with a single-cell lifestyle (Komárek et al. 2011, 2014). This has led to discrepancies between microscopic and genetic methods in identifying dominant taxa (Albrecht et al. 2017; MacKeigan et al. 2022). Because of the limited resolution and database representation of many colony morphotypes (Komárek et al. 2014), as well as high similarity among picocyanobacteria on the 16S rRNA gene, caution must be used when interpreting lifestyle characteristics from molecular data. In addition, the formation of microcolonies by strains largely recognized as single-celled (e.g., *Cyanobium*) has been described in lake systems (Huber et al. 2017), with studies suggesting that microcolony formation may be a strategy to avoid predation (Jezberová and Komárková 2007; Callieri et al. 2016) or as a response to changes in the light environment (Callieri et al. 2011) and can help sustain growth in low-nutrient conditions (Xiao et al. 2018). Meanwhile, colony-forming groups are also suggested to exhibit single-cell lifestyle stages (Komárková and Šimek 2003). While crossover exists in the life-style preferences of these picocyanobacteria, it is recognized that there are differences between the true colonial and single-cell strains that play out at the level of community ecology (Callieri et al. 2012).

In addition to the overlapping lifestyle structure between single-cell and colony-forming species, the presence of colony-forming picocyanobacteria may be obscured by the methods used to enumerate the nanophytoplankton and picophytoplankton size fractions. Flow cytometry (FCM) has long been a standard method for enumerating picocyanobacteria (Olson et al. 1988), utilizing autofluorescence characteristics of phycoerythrin, or phycocyanin, as well as chlorophyll *a* (Chl *a*), interrogating individual cell "events" that pass by a laser. These events can be either single cells or entire colonies, however, limiting the ability of flow cytometry to accurately count picocyanobacteria in complex communities. Colonies can therefor easily be overlooked and counted as individual cells if analysis is not conducted to separate the single-cell and colony populations. Some studies have succeeded in counting microcolonies among single-cell populations (Callieri et al. 2016); however, measurement fluidics can partially break up colonies (Rutten et al. 2005), providing neither an accurate number of cells or characteristics of the undisturbed colonies. While epifluorescence microscopy counting can resolve colony morphology, it requires training and standard operational protocols for correct identification and counting of colonial forms.

Correctly characterizing the species composition is important for understanding how the community interacts with the nutrient environment. Specifically, required nitrogen (N) can be attained in a variety of ways with preferred sources differing between species and strains (Berg et al. 2003). Available inorganic/organic N sources are additionally associated with and can influence species composition. Most marine *Synechococcus* can utilize ammonium (NH_4) and nitrate (NO_3) and few strains are recognized to only grow on NH_4 (Fuller et al. 2003). Many *Prochlorococcus* do not have the ability to use NO_3 or nitrite

(NO_2) (Moore et al. 2002). For certain strains, high concentrations of NH_4 may also inhibit NO_3 uptake, when there is otherwise no preference exhibited or growth advantages given (Collier et al. 2012; Alegria Zufia et al. 2021). As important contributors to marine total amino acid uptake (Michelou et al. 2007), there is also variability in the number of acquisition genes in *Synechococcus* and *Prochlorococcus*, with many *Prochlorococcus* lacking amino acid transporter genes (Muñoz-Marín et al. 2020). Growth on urea is reported for both *Synechococcus* and *Prochlorococcus* but growth response varies between strains (Moore et al. 2002). While data are more limited, some freshwater picocyanobacteria do not appear to utilize amino acids (Salcher et al. 2013), while urease genes have been identified in some strains inferring utilization of urea (Cabello-Yeves et al. 2018).

Nutrient acquisition strategies of natural communities can be explored at the single-cell level using secondary-ion mass spectrometry (SIMS) and nanoscale secondary-ion mass spectrometry (NanoSIMS) to acquire species-specific rates and metabolic variability within populations. In the North Atlantic and North Pacific, *Synechococcus* exhibit a preference for reduced forms of N, NH_4, and urea, while leucine uptake was very low compared to picoeukaryotes and *Prochlorococcus* (Berthelot et al. 2019, 2021). In the brackish Baltic Sea, *Synechococcus* can have the highest NH_4 consumption in the phytoplankton community with uptake rates similar to co-occurring diatoms (Klawonn et al. 2019).

In the Baltic Sea, picocyanobacteria can contribute up to 50% of the primary production (Stal et al. 2003). They are most abundant during summer when N limiting conditions prevail and their small size give them competitive advantages compared to larger phytoplankton (Legrand et al. 2015). Picocyanobacteria genera with a single-cell lifestyle such as *Synechococcus* and *Cyanobium* are recognized as important contributors to the microbial assemblages (Celepli et al. 2017; Alegria Zufia et al. 2022). However, colony-forming picocyanobacteria, which can dominate annual phytoplankton abundances in brackish lagoons (Albrecht et al. 2017) and compose up to 50% of phytoplankton biomass in the Gotland Basin (Hajdu et al. 2007), have received little attention. This stands in contrast with freshwater systems where they are both abundant and have been extensively studied (Somogyi et al. 2020). While recognition of colony-forming cyanobacteria in the Baltic Sea is not new (Laamanen 1997; Hajdu et al. 2007), investigations studying their presence and dynamics remain limited (Łysiak-Pastuszak et al. 2012) and they are often overlooked, with emphasis placed on contrasting filamentous and single-cell lifestyles.

In this study, we investigated N and C substrate uptake preferences of picocyanobacteria growing in the central Baltic Sea during late summer (August and September). We used dual stable isotope labeling (^{13}C and ^{15}N) to measure single-cell N assimilation and C fixation using total community uptake rates with isotope ratio mass spectrometer (IRMS) as well as NanoSIMS analysis to understand the contribution of picocyanobacteria to

total uptake. Furthermore, we investigated uptake dynamics between free and colonial picocyanobacteria lineages and explored the seasonal contribution of colony-forming species to phytoplankton abundance over six consecutive years at an offshore station in the central Baltic Sea. This study revealed how diversity in Baltic Sea picocyanobacteria assemblage can influence the contribution to nutrient flow and specifically investigates colony-forming picocyanobacteria, a group of picophytoplankton that are largely understudied in brackish systems.

Methods

Sampling and experiment setup

Sampling and nutrient uptake experiments were conducted on August 11, 2020 and September 14, 2020. Seawater was collected from 1 m depth at the Linnaeus Microbial Observatory (LMO) station, located 10 km offshore from Kårehamn, Sweden (56°55.8540′N, 17°3.6420′E). The LMO is a long-term time series station that has monitored abiotic and biotic factors in the central Baltic Sea at least monthly since 2011 (e.g., Legrand et al. 2015; Bunse et al. 2019; Hagström et al. 2021; Fridolfsson et al. 2023). Seawater for the experiment was collected with a 5-liter Ruttner sampler and mixed in a 70-liter opaque barrel. Accompanying water column profiles of conductivity, temperature, and depth were measured with a CTD probe (AAQ 1186-H, Alec Electronics). Collected seawater was taken to the field station in Kårehamn where it was filtered through a 200-μm mesh to remove large grazers. For each of the four isotope manipulation experimental groups (NH_4, NO_3, amino acids, urea) and the control group (no nitrogen/carbon addition), five acid-washed 0.5-liter polypropylene bottles were filled with the seawater, leaving no headspace for air. To prevent contamination of the control group with any stable isotope, we filled and sampled control group bottles in a separate part of the lab from where the stable isotope manipulations and sampling occurred. Control bottles were immediately closed while the isotope manipulation bottles were inoculated with stable nitrogen and carbon isotopes. Bottles for the NH_4 group received a final concentration of 0.5 μM ammonium-^{15}N chloride (^{15}N-NH_4; Sigma-39466-62-1) and 195 μM sodium bicarbonate-^{13}C (^{13}C-HCO_3; Sigma-87081-58-1). The NO_3 group bottles received 0.05 μM sodium nitrate-^{15}N (^{15}N-NO_3; Sigma-7631-99-4) and 195 μM ^{13}C-HCO_3. The urea group received 0.5 μM of dual Urea-^{13}C,^{15}N$_2$ (Sigma, 58069-83-3). The amino acid group received 0.5 μM dual ^{13}C,^{15}N cell free amino acid mix (Sigma, 767964). For each of the five experiment groups, a single bottle was kept for immediate measurement ($T0$) while an additional four bottles for each group were strapped to a 1 m × 1 m metal grid and returned offshore for a 5-h (12:00–17:00 on August 11; 12:30–17:30 on September 14) in situ incubation, with all bottles suspended at 1 m depth. After 5-h, these bottles were also brought back to the lab and harvested. Temperature and light intensity were monitored throughout the incubations at 15-min intervals using Hobo loggers (Onset) attached to the grid structure.

Initial ($T0$) samples of the seawater were collected for NH_4, nitrite + nitrate ($NO_2 + NO_3$), phosphate (PO_4), and silica (SiO_2) concentration, urea, dissolved free amino acids (DFAA), dissolved inorganic carbon (DIC), particulate organic carbon (POC), particulate organic nitrogen (PON), Chl a, flow cytometry cell enumeration, light microscopy, elemental analyzer (EA)-IRMS, and community DNA. After 5-h ($T5$), samples were collected for DIC, flow cytometry, EA-IRMS, and NanoSIMS from the incubation bottles.

Nutrients, DIC, and POC/PON

Nutrient samples were collected in acid washed 500-mL PET containers and frozen at −20°C. Dissolved NO_2, $NO_2 + NO_3$, SiO_2, and PO_4 concentrations were measured with a four-channel continuous flow analyzer (San++, Skalar) using standard colorimetric methods (Grasshoff et al. 2009) in the Zilius Lab (Klaipeda University). NO_3 was calculated as the difference between $NO_2 + NO_3$ and NO_2. NH_4 was measured on a DR3900 spectrophotometer (Hach) instrument using standard protocols (Valderrama 1995). Urea concentrations were measured by direct method using color developing reagent (COLDER) following Mulvenna and Savidge (1992). Determination of the DFAA was conducted according to (Parsons et al. 1984) using a FLUOstar Omega plate reader (BMG Labtech).

Samples for ^{13}C DIC were collected in 12-mL septum capped vials (Exetainers, Labco) and preserved with 0.8% $ZnCl_2$ w/v final concentration and stored at room temperature before being shipped to UC Davis Stable Isotope Facility (https://stableisotopefacility.ucdavis.edu/) for processing using a GasBench II system interfaced to a Delta V Plus EA-IRMS (Thermo Scientific).

POC and PON were collected at $T0$ by filtering 500-mL seawater onto duplicate precombusted GF/F filters. Samples were immediately frozen at −20°C until further processing. Following, samples were dried overnight in an oven at 60°C before being measured on a Perkin Elmer 2400 CHN organic elemental analyzer.

Chl a and flow cytometry

Chl a was sampled by filtering 250-mL seawater from the bottles on 25-mm GF/F filters and extracting Chl a from the filter in 4-mL 90% EtOH overnight in borosilicate culture tubes. Filters were removed from the tubes and the extracted Chl a was measured on a Trilogy Fluorometer (Jespersen and Christoffersen 1987). Flow cytometry samples for photosynthetic picoplankton counting were collected in cryotubes and fixed with 1% final concentration grade I glutaraldehyde solution (Sigma, G5882). Samples were immediately frozen at −80°C until analysis. Cell enumeration was conducted with two technical replicates counted on a Cube8 flow cytometer (Partec) using natural fluorescence and scattering characteristics. Picocyanobacteria and photosynthetic picoeukaryotes

were identified using forward scatter as a proxy for cell size and red fluorescence from the 488-nm laser as a proxy for Chl *a* content. Orange fluorescence was used as a proxy for phycoerythrin pigment present in picocyanobacteria cells. Population gating and abundance measurements were performed in FCSalyzer 0.9.22.

Biomass and cell counts, cell size

Samples for phytoplankton and picocyanobacteria colony enumeration were preserved with acid Lugol's solution (Utermöhl 1958), and phytoplankton were identified to genus or species level using an inverted microscope (Nikon TMS) at 400× magnification. Colony sizes were approximated as 50, 100, and 200 cells. Colonies smaller than ∼ 50 cells were not included in the analysis. Cell counts were converted to carbon biomass using the Manual for Marine Monitoring in the COMBINE program of the Helsinki Commission (HELCOM) carbon conversion calculations (HELCOM 2021). In addition to the samples collected during the experiments, colony-forming picocyanobacteria were also counted between 2015 and 2020 from bi-monthly sampling at LMO. Cell size of single-cell picocyanobacteria from the experiments were determined using epifluorescence microscopy (Olympus BX50) at 1000× magnification using the samples prepared for NanoSIMS (*see* below). Images were taken of each *T*0 replicate, and cell length was measured using ImageJ software (Schneider et al. 2012).

DNA and amplicon sequencing

Samples for DNA extraction were collected by filtering 500-mL of seawater through a 0.22-*μ*m Sterivex membrane filter. In August, duplicate samples were collected and in September triplicate samples were collected. The filters were stored at −80°C until extraction. Samples were extracted using the FastDNA™ SPIN Kit for Soil from MP Biomedicals Inc. according to manufacturer's instructions with the addition of a 1-h incubation with proteinase-K (20 mg mL⁻¹, final concentration) at 55°C. A two-step PCR amplification was performed, as described by Mattsson et al. (2021), targeting the V3–V4 region of the 16S rRNA gene using the 341F and 805R primers (Herlemann et al. 2011). Samples were pooled at equal concentrations and were sequenced using MiSeq Illumina technology (2 * 300 bp) at the National Genomics Infrastructure in Stockholm.

Data analysis of amplicon libraries

The amplicon libraries were analyzed using the nf-core/Ampliseq v.1.2 (Straub et al. 2020) pipeline using DADA2 1.10.0 (Callahan et al. 2016) implemented in QIIME2 v2019.10.0 (Bolyen et al. 2019). The initial taxonomic assignments were performed using the q2-feature-classifier plugin (Bokulich et al. 2018), trained on Silva v132 sequences. The dataset was then filtered to only contain Cyanobacteria. Samples were then rarified to 1361 sequence reads corresponding to the sample with the least reads.

The phylogenetic placement tree was created using an in-house Python (v.3.9) workflow. Cyanobacterial amplicon sequence variants (ASVs; defined as individual sequences, no clustering) were first blasted in NCBI to retrieve the closest DNA sequences as references. For these reference sequences, as well as additional cyanobacterial sequences, a first multiple sequence alignment was obtained with Muscle (v3.8) using the reference sequences (maximum iteration: 2). The alignment was trimmed to 1370 bp with TrimAl (v1.4) to obtain a better quality of the final reference tree, as described by Capella-Gutiérrez et al. (2009), with a minimum overlap of positions = 0.55 and a minimum percentage of "good positions" = 60. A maximum-likelihood tree was inferred using the edge-linked partition model in IqTree (Nguyen et al. 2014) with 1000 bootstraps obtained with ultrafast bootstrap support (Hoang et al. 2017). The parameter model was obtained by using the built-in function Modelfinder (Kalyaanamoorthy et al. 2017). To place the ASVs in the reference phylogenetic tree, an alignment between the query FASTA sequences and the references was obtained with Hmmalign (HMMER v3.1. b2; http://hmmer.org). EPA-ng (v0.3.8) was then performed with the same model as used in IqTree, as suggested by Barbera et al. (2018). Finally, to visualize the phylogenetic placement, Gappa (v 0.7.1; Czech et al. 2020) was used to analyze and convert the jplace file into a text newick file. The phylogenetic placement tree was visualized using the Interactive Tree of Life (itol.embl.de; Letunic and Bork 2019).

Measurement of community C and N uptake

To measure bulk community ¹³C and ¹⁵N uptake at *T*0 and *T*5, 100–200 mL seawater from the incubation bottles was filtered to collect biomass onto GF/F filters in either duplicate or triplicate samples. Filters were dried at 60°C overnight before being sent to the ISOGOT facility (https://www.gu.se/en/earth-sciences/isogot-infrastructure-for-isotope-determination-within-earth-system-sciences) at the University of Gothenburg for analysis and measured on a coupled elemental analyzer isotope ratio mass spectrometer (EA-IRMS).

Measurement of single-cell C and N uptake

NanoSIMS samples for single-cell ¹³C and ¹⁵N uptake measurements were fixed with 2% paraformaldehyde final concentration and kept at room temperature in the dark for 2-d before filtering 15-mL onto 0.2-*μ*m isopore filters. Filters were examined using fluorescence microscopy with excitation (546 nm) and emission (585 nm) filter to excite phycoerythrin, identifying regions of interest (ROIs) containing colony-forming (*Aphanothece parallelliform*, *Aphanothece smithii*, and other unclassified colony-forming picocyanobacteria) and single-cell picocyanobacteria, as well as create surface maps of the filter area using a camera mounted to the microscope. Filters were cut to 1 cm × 1 cm squares containing the ROIs and mounted onto a 10-mm stainless steel sample disc with carbon tape before gold sputter coating. Sample analysis was performed on a Cameca NanoSIMS 50L.

ROIs were identified for investigation on the instrument using the sample surface maps. Analyses were conducted over a field of 50×50, 30×30, 20×20, and $10 \times 10\,\mu m$ with 256×256 pixel resolution. Cesium primary ion implantation dosage was between 17 and 22 nA. Between 5 and 15 planes were collected for each analysis with a dwell time of 1.3 ms per pixel. Images were recorded for $^{12}C^{12}C$, $^{12}C^{13}C$, $^{12}C^{14}N$, and $^{12}C^{15}N$ simultaneously and image analysis was performed in WinImage software (Cameca). Regions of interest were manually selected from the images with log scale image coloration.

Data analysis

From the EA-IRMS and NanoSIMS analysis, isotopic fractional percent abundances of ^{13}C and ^{15}N ($A^{13}C$, $A^{15}N$) were used to calculate the C- and N-specific uptake rates (h^{-1}).

$$A^{13}C = \frac{^{13}C^{12}C^-}{^{13}C^{12}C^- + {}^{12}C^{12}C^-} \times 100 \qquad (1)$$

$$A^{15}N = \frac{^{12}C^{15}N^-}{^{12}C^{15}N^- + {}^{12}C^{14}N^-} \times 100 \qquad (2)$$

where $^{13}C^{12}C^-$, $^{12}C^{12}C^-$, $^{12}C^{15}N^-$, and $^{12}C^{14}N^-$ are the abundances of ^{13}carbon-^{12}carbon, ^{12}carbon-^{12}carbon, ^{12}carbon-^{15}nitrogen, and ^{12}carbon-^{14}nitrogen molecules, respectively. Following Berthelot et al. (2021), C-specific fixation (h^{-1}) and N-specific uptake rates (h^{-1}) were calculated with:

$$\text{Element-specific uptake} = \frac{A_{\text{target}} - \overline{A}_{t0}}{A_{\text{source}} - \overline{A}_{t0}} \times \frac{1}{t} \qquad (3)$$

where A_{target} is the isotopic percent abundance of the community biomass (EA-IRMS) or single-cell (NanoSIMS), A_{source} is the respective isotope percent abundance of the inoculated source water at the beginning of the experiment and $\overline{A}_{t0}$ is the isotope percent abundance of biomass at the beginning of the experiment, and t is the time since the beginning of the experiment, at which biomass/cells are harvested.

Rates for the total community C fixation and N uptake (nmol $L^{-1}\,h^{-1}$) were calculated from EA-IRMS $A^{13}C$ and $A^{15}N$ using:

$$\text{Community-specific uptake} = \frac{A_{\text{POM}} - \overline{A}_{t0}}{A_{\text{source}} - \overline{A}_{t0}} \times \frac{\text{POM}}{t} \qquad (4)$$

where POM (nmol L^{-1}) is the concentration of total particulate organic C or N in the GFF filter biomass, A_{POM} is the isotopic percent abundance of ^{13}C or ^{15}N in the total particulate organic C or N.

For individual picocyanobacteria cells, cell-specific uptake rates (nmol cell$^{-1}\,h^{-1}$) from NanoSIMS were calculated with:

$$\text{Cell-specific uptake} = \frac{A_{\text{cell}} - \overline{A}_{t0}}{A_{\text{source}} - \overline{A}_{t0}} \times \frac{Q_{\text{cell}}}{t} \qquad (5)$$

where Q_{cell} is the cellular quota of C or N for an individual cell. Q_{cell} was calculated for free cells using an average of *Synechococcus* strain cellular C quotas from literature found by Alegria Zufia et al. (2021) at 246.5 fgC cell^{-1}. For colony-forming picocyanobacteria, taxon-specific C content was calculated following the HELCOM manual (HELCOM 2021). Cellular N quotas for free cells were based on an quota in picocyanobacteria observed by Baer et al. (2017) in the North Atlantic Ocean and used by Berthelot et al. (2021). Because there were no measurements of N cell quotas for colonial picocyanobacteria, we used a C : N ratio of 6.6 (Redfield 1958). Single-cell and colony-forming biomass-specific uptake rates (nmol $L^{-1}\,h^{-1}$) were then calculated using cell abundances of the free and colony-forming cells.

Results

Environmental conditions and phytoplankton abundances

The experiments were conducted during typical late summer conditions in the central Baltic Sea and incubated in situ. Between the August and September experiments, the water temperature had dropped from 19.4°C to 14.3°C (Table 1). PO_4 concentrations were similar (0.38–0.40 μM) during both experiments while NH_4, urea, and DFAA were higher in August (0.76, 0.99, and 0.87 μM), than in September (0.36, 0.62, and 0.36 μM), respectively. Concentrations of $NO_3 + NO_2$ and SiO_2 were lower in August (0.30 and 8.61 μM) compared to September (0.56 and 11.07 μM), respectively. While day length was longer in August (15 h compared to 13 h), phytoplankton had higher light exposure during the experiment in September. Phytoplankton biomass was substantially higher in August (186.1 mg C m^{-3}) compared to September (6.1 mg C m^{-3}; Table 1). The cyanobacterial community was dominated by the filamentous cyanobacteria *Nodularia spumigena* and *Aphanizomenon flos-aquae* (Supporting Information Table S1). Chl *a* was 3.3 $\mu g\,L^{-1}$ in August and 2.1 $\mu g\,L^{-1}$ in September.

The abundances of picophytoplankton differed largely between the experiments. Photosynthetic picoeukaryote abundances were higher in August than September while single-cell picocyanobacteria over twice as abundant in September (2.6×10^5 cells mL^{-1} compared to 1.1×10^5 cells mL^{-1}). Colony-forming picocyanobacteria were abundant in August with 1.7×10^3 cells mL^{-1}, but almost absent in September with only 2.9 cells mL^{-1} (Table 1). Microscopy counts in August revealed *Aphanothece paralleliformis* were present in addition to *Woronichinia* and *Cyanodictyon* (Supporting Information Table S1). Abundance of *Aphanocapsa*-like cells were highest among the colony-forming species at 1.1×10^3 cells mL^{-1}. In September, the picophytoplankton were largely composed of single-cell picocyanobacteria. Very few *Aphanocapsa*-like

Table 1. Environmental conditions during the two experiments in 2020. Temperature (°C) and salinity were measured in situ. NH_4, $NO_3 + NO_2$ (μM), PO_4 (μM), SiO_2 (μM), Chl a (μg L^{-1}), phytoplankton carbon (μg C L^{-1}), picoeukaryotes (cells mL^{-1}), single-cell picocyanobacteria (Pcy) (cells mL^{-1}), and colony-forming picocyanobacteria (cells mL^{-1}) were measured from the experimental bottles (data presented as mean $\pm$ SD). For August and September, respectively, NH_4 $n = 3$, 3; NO_3 $n = 3$, 3; PO_4 $n = 3$, 3; SiO_2 $n = 3$, 3, Chl a, $n = 3$, 3 phytoplankton $n = 1$, 1; picoeukaryotes $n = 3$, 3; single-cell picocyanobacteria $n = 3$, 3; colony-forming picocyanobacteria $n = 1$, 1.

	Aug	**Sept**
Date	Aug 11, 2020	Sept 14, 2020
Temperature (°C)	19.3	14.3
Salinity (PSU)	7.15	7.15
Average light (μmol photon m^{-2} s^{-1})	67 ± 42	111 ± 177
NH_4 (μM)	0.76 ± 0.44	0.36 ± 0.01
$NO_3 + NO_2$ (μM)	0.30 ± 0.02	0.56 ± 0.02
Urea (μM)	0.99 ± 0.26	0.62 ± 0.15
DFAA (μM)	0.87 ± 0.02	0.36 ± 0.07
PO_4 (μM)	0.38 ± 0.01	0.40 ± 0.00
SiO_2 (μM)	8.61 ± 0.87	11.07 ± 0.03
Chl a (μg L^{-1})	3.03 ± 0.03	2.08 ± 0.25
Phytoplankton (μg C L^{-1})	186.0	6.1
Picoeukaryotes (cells mL^{-1})	3.2×10^4	2.8×10^4
Single-cell Pcy (cells mL^{-1})	1.2×10^5	2.6×10^5
Colony-forming Pcy (cells mL^{-1})	1.7×10^3	2.9

cells could still be observed with a decrease in abundance by three orders of magnitude. Other colony-forming species were either not present or only rarely observed. The cell size of single cells was similar in August and September, with averages of 1 μm cell diameter (Supporting Information Fig. S1). In both August and September, phycocyanin-rich picocyanobacteria were not detected with flow cytometry and were not explored further.

Cyanobacteria community composition 16S rRNA gene amplicon sequencing

To investigate the diversity of picocyanobacteria present during our study, we used 16S rRNA for a broad but coarse perspective of phylogeny. ASVs were placed in a phylogenic tree constructed from reference 16S rRNA gene sequences of cyanobacteria species common to the Baltic Sea as well as references having the highest BLASTn identity scores with our ASVs (Supporting Information Fig. S2). The tree presents a clear division between Synechococcales and filamentous cyanobacteria. However, the placement of branches within these groups should be interpreted cautiously due to the limitations of the 16S rRNA gene at this level of taxonomic resolution. Within the tree, *Aphanothece* spp. were divided among two

separate regions of the tree. Three of the *Aphanothece* spp. representatives branched among the Synechococcales while two representatives were closer to filamentous cyanobacteria and other colony-forming picocyanobacteria.

A total of 15 ASVs were mapped among Synechococcales while 27 ASVs mapped among filamentous cyanobacteria and 8 ASVs mapped to other cyanobacteria (Supporting Information Fig. S2). Synechococcales composed 25% of the total cyanobacterial reads in August and 64% in September (Supporting Information Table S2). Among the experimental replicate samples, there were 29 ± 9 cyanobacterial ASVs observed in August while only 16 ± 2 were present in September (Supporting Information Table S2). Among these ASVs, 10 ± 0 and 12 ± 2 were identified as Synechococcales in August and September, respectively.

Differences in the picocyanobacteria assemblage can be further explored by looking at the relative contributions of individual ASVs. Twenty ASVs were identified as picocyanobacteria based on the reference sequence they mapped nearest to in the phylogenic tree. Fifteen of these were within Synechococcales and five were among other cyanobacteria phyla (Fig. 1; Supporting Information Fig. S1). The ASVs exhibited individual differences in mean proportions between the two experiments (Fig. 1). Ten picocyanobacteria ASVs were only observed in either August or September. Of the five observed only in August, two mapped to *Vampirovibrio*, two mapped to *Synechococcus* and *Cyanobium*, and one mapped equally between *Aphanothece sacrum* and *Planktothrix agardhii*. Four ASVs were preferentially observed in August with a > 33% preference to community contribution in August, including *Vampirovibrio* and *Synechococcus*. Three ASVs showed similar mean proportions in September and included *Synechococcus* and *Aphanothece hegewaldii*. The five ASVs observed in September only, all mapped to *Synechococcus* and *Cyanobium*. Collectively, the sequences preferentially observed in August made up 53% of the mean August picocyanobacteria amplicon libraries while those preferentially observed in September only made up 40% of the mean September amplicon libraries.

Seasonality and contribution of colony-forming picocyanobacteria

To address the contribution of colony-forming picocyanobacteria to the total phytoplankton community in the central Baltic Sea, 6-yr data (2015–2020) from the LMO time series was investigated. Abundances were highly variable between years, having up to two orders of magnitude or more difference for similar dates between years (Fig. 2a). For the majority of the year, cell abundances remained below 1×10^3 cells mL^{-1}. However, the average abundance quickly increased after day 150, and peaked in July at $6 \times 10^4 \pm 1.0 \times 10^5$ cells mL^{-1}. The highest total abundance observed was in July 2018 with 2.6×10^5 cells mL^{-1}. Colonies were periodically not observed throughout the year; however,

(a)   (b) Preferential Observation   (c) Relative abundance (%)

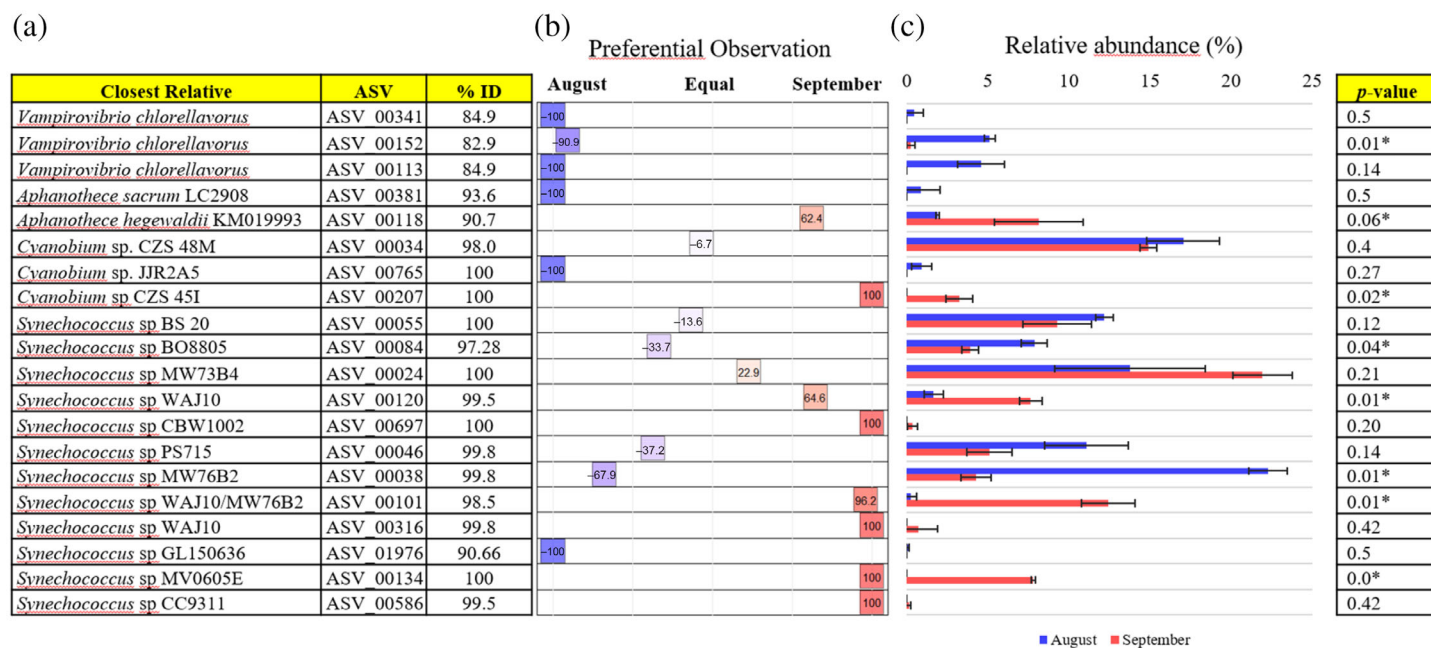| Closest Relative	ASV	% ID	August	Equal	September	p-value
Vampirovibrio chlorellavorus	ASV_00341	84.9	−100			0.5
Vampirovibrio chlorellavorus	ASV_00152	82.9	−90.9			0.01*
Vampirovibrio chlorellavorus	ASV_00113	84.9	−100			0.14
Aphanothece sacrum LC2908	ASV_00381	93.6	−100			0.5
Aphanothece hegewaldii KM019993	ASV_00118	90.7			62.4	0.06*
Cyanobium sp. CZS 48M	ASV_00034	98.0		−6.7		0.4
Cyanobium sp. JJR2A5	ASV_00765	100	−100			0.27
Cyanobium sp CZS 45I	ASV_00207	100			100	0.02*
Synechococcus sp BS 20	ASV_00055	100		−13.6		0.12
Synechococcus sp BO8805	ASV_00084	97.28		−33.7		0.04*
Synechococcus sp MW73B4	ASV_00024	100		22.9		0.21
Synechococcus sp WAJ10	ASV_00120	99.5			64.6	0.01*
Synechococcus sp CBW1002	ASV_00697	100			100	0.20
Synechococcus sp PS715	ASV_00046	99.8		−37.2		0.14
Synechococcus sp MW76B2	ASV_00038	99.8	−67.9			0.01*
Synechococcus sp WAJ10/MW76B2	ASV_00101	98.5			96.2	0.01*
Synechococcus sp WAJ10	ASV_00316	99.8			100	0.42
Synechococcus sp GL150636	ASV_01976	90.66	−100			0.5
Synechococcus sp MV0605E	ASV_00134	100			100	0.0*
Synechococcus sp CC9311	ASV_00586	99.5			100	0.42

■ August ■ September

Fig. 1. Identity and observation of picocyanobacteria ASVs during the experiments in August and September. (**a**) Percent identity of ASVs to the closest relative present in the phylogenic tree (Supporting Information Fig. S1). (**b**) The preferential observation of ASVs during the two experiments based on mean relative abundance. (**c**) The mean relative abundance of each ASV to the picophytoplankton community during the respective experiments. Means for August and September are $n = 2, 3$, respectively. Error bars indicate $\pm$ SD.

between days 190 and 290 colonies were always observed. The colony composition changed throughout the year, with major contributor most often in the genera *Anathece*, *Aphanothece*, *Aphanocapsa*, *Cyanodictyon*, and *Woronichinia* (Supporting Information Fig. S3). The contribution of colony-forming picocyanobacteria to total phytoplankton biomass also varied throughout the year, with the lowest contribution ($< 1\%$) in the spring between March and May, while the highest contribution was in July and August, where they averaged $6\% \pm 9\%$ and $5\% \pm 5\%$, and maximally accounted for 27% of the carbon (Fig. 2b).

Community uptake rates

During the experiments, the addition of $^{15}NH_4$, $^{15}NO_3$, ^{15}N urea, and ^{15}N DFAA increased nutrient concentrations by 10%, 14%, 4%, and 6% in August and 14%, 9%, 8%, and 14% in September, respectively. Phytoplankton community uptake rates of inorganic (NH_4 and NO_3) and organic (urea and DFAA) forms of N as well as DIC were measured using IRMS. C-specific fixation rates were similar for both experiments (Fig. 3a). N-specific uptake was different between August and September (Fig. 3b). In August, significant differences in uptake were observed (Kruskal–Wallis, $p < 0.01$), with NH_4 having the highest rate (1.2×10^{-2} h^{-1}) and NO_3 having the lowest rate (2.4×10^{-3} h^{-1}). Urea uptake was higher than DFAA but lower than NH_4. Differences between these substrates were all significant by pairwise testing (Wilcox, $p < 0.05$). In September, uptake rates of all N substrates were higher than in August, except for DFAA, which was lower (Wilcox, $p < 0.05$). NH_4 had the highest uptake rate, followed by urea. NO_3 uptake was higher than that of DFAA (Wilcox, $p < 0.05$).

Single-cell uptake rates

NanoSIMS image analysis was used to study the uptake rates of single-cell and colony-forming picocyanobacterial cells. In total, we measured the uptake rates of 3378 cells and 1001 cells in August and September, respectively. During the August experiment, images of single-cell and colony-forming cells were collected while the shift in picocyanobacteria community lead to only single cells being imaged in September. There were some incongruencies between our light microscopy and fluorescence microscopy/NanoSIMS data, namely the presence of *A. smithii*. Due to the limitations of light microscopy at 40× for identifying colony-forming species, it is likely that similar shaped morphotypes were collectively classified as *Aphanocapsa* sp. The fluorescent microscopy used for identifying cells for NanoSIMS, however, verified the presence of *A. smithii*. *A. smithii* and *A. paralleliformis* dominated the colony-forming picocyanobacteria, but images with other unclassified colony morphology were also captured and were included in the calculations for colony cell-specific uptake (*see* below). Colonies varied in size (~ 50–2000 cells) and for most images only a fraction of the colony was analyzed.
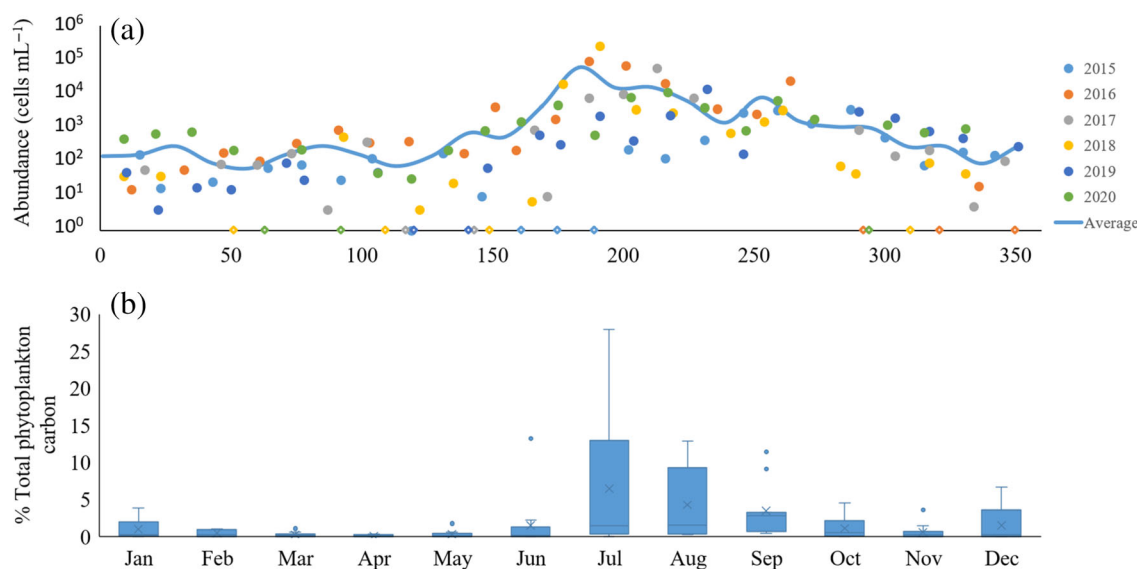
Fig. 2. (**a**) Abundances of colony-forming picocyanobacteria at the Linnaeus Microbial Observatory (LMO) station throughout the year (Julian date) between 2015 and 2020. Open diamonds indicate sampling dates where no colonies were observed. Average line indicates data at 2-week intervals. (**b**) Monthly contribution of colony-forming picocyanobacteria to total phytoplankton carbon between 2015 and 2020. In the boxplot, × indicates the mean values while ∘ indicates outliers.
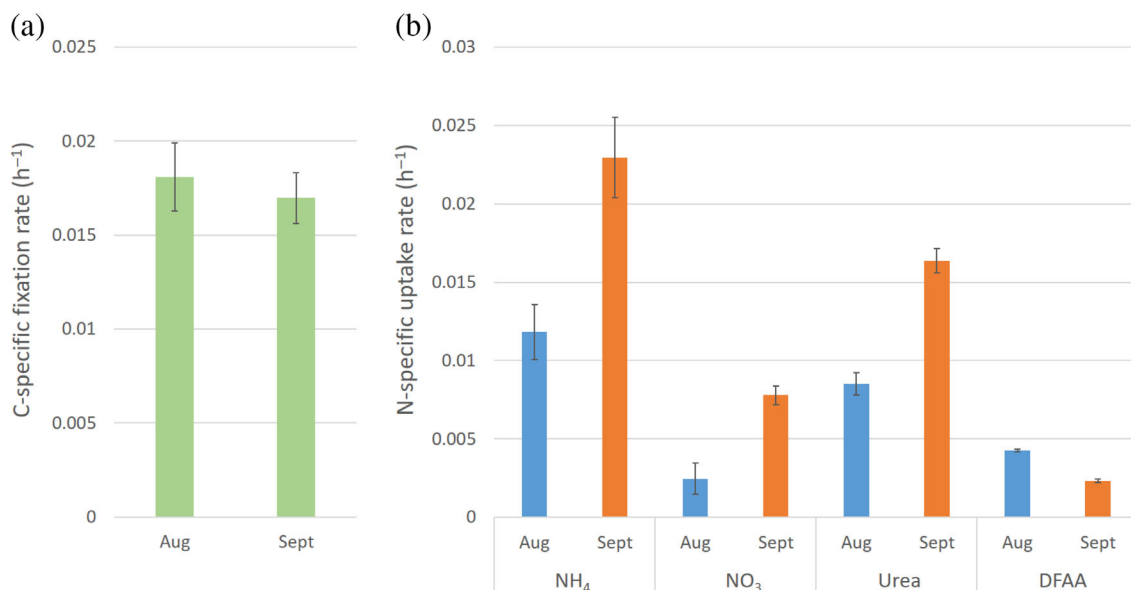

Fig. 3. Community-level uptake rates during experiments in August and September 2020. (**a**) Carbon-specific fixation rates. (**b**) Nitrogen-specific uptake rates of NH_4, NO_3, urea, and DFAA. Error bars represent $\pm$ 1 standard deviation.

At the individual cell level, average C-specific fixation rates ranged between 3.3×10^{-2} h^{-1} (single-celled picocyanobacteria in September) and 7.1×10^{-3} h^{-1} (*A. smithii*). Between the three groups in August, the average was higher for single-celled picocyanobacteria than *A. smithii* (Wilcox, $p < 0.05$; Fig. 4a). In September, C fixation rates for single picocyanobacteria were higher than in August (Wilcox, $p < 0.01$). For N-specific uptake rates, averages ranged between 3.8×10^{-2} h^{-1} (single-celled

picocyanobacteria NH_4 in September) and 5.0×10^{-4} h^{-1} (*A. smithii* NO_3). There were significant differences in N-specific uptake rates for single picocyanobacteria in August (Kruskal–Wallis, $p < 0.01$) as well as in September (Kruskal–Wallis, $p < 0.01$; Fig. 4b). Single-cell picocyanobacteria took up NH_4 at the highest rate, followed by urea, AA and NO_3 (for all Wilcox tests, $p < 0.05$). Comparing single-cell to colony-forming lifestyles, differences were observed among NH_4 uptake (Kruskal–
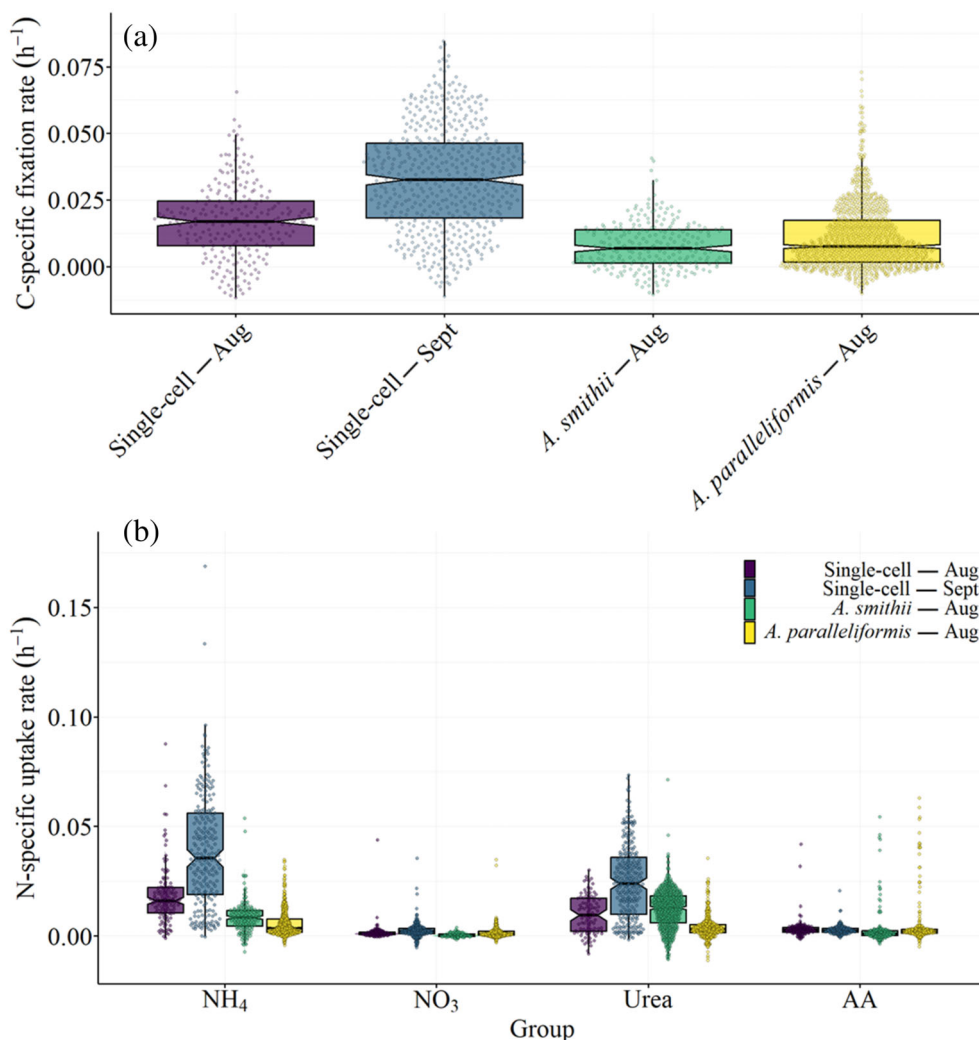
Fig. 4. (**a**) Cellular carbon-specific fixation rates of picocyanobacteria groups observed in this study. (**b**) Nitrogen-specific uptake rates of four N substrates (NH_4, NO_3, Urea, AA) by the picophytoplankton investigated in this study. Circles represent individual cells measured by NanoSIMS. Box plot represents the median, upper and lower quartiles of all sampled cells for each picophytoplankton group.

Walis, $p < 0.05$) with single cells having a higher uptake rate than *A. paralleliformis* (Wilcox, $p < 0.05$). Rates also differed for urea, with single-cell picocyanobacteria having higher uptake than *A. paralleliformis* (Wilcox, $p < 0.05$). Comparing uptake between the two experiments, single-cell picocyanobacteria had higher NH_4 and urea uptake in September than in August (Wilcox, $p < 0.05$).

C-specific fixation and N-specific uptake rates were extrapolated to biomass-specific rates by multiplying the average values by biomass measurements during each experiment and known cellular C/N quotas, respectively (Table 2; Eq. 4, 5). Community-specific C fixation was more than double in August compared to September. Community-specific N uptake rates were higher in August for NH_4, urea, and DFAA, but higher in September for NO_3. Single-cell picocyanobacteria had higher uptake for all N substrates in September than in

August, with NH_4 and urea having the largest differences. Single cells contributed greater to the total community uptake of all substrates in September, with the largest difference in urea uptake increasing from 4% to 40% of the community uptake. Single cells also contributed greater to the C fixation rates in September, increasing from 4% to 36%. Colony-forming picocyanobacteria, which were only observed in August, had a much lower contribution to N uptake and C fixation, and contributed similarly to NH_4, urea, and DFAA uptake. However, all uptake rates of colony-forming picocyanobacteria contributed to < 1% of the total community uptake.

Discussion

Late summer in the central Baltic Sea is characterized by a decrease in phytoplankton biomass, bacterial production, and

Table 2. Single-cell and colony-forming specific uptake rates (from NanoSIMS) of picophytoplankton (Pcy) utilizing nitrogen substrates (NH_4, NO_3, urea, and DFAA) and carbon fixation rates during the August and September experiments. Values are compared to the total community-specific uptake (from IRMS) and fixation rates for an assessment of proportional contribution. Error is presented as ± 1 SD of the mean.

	NH_4		NO_3		Urea		Amino acid		Carbon	
	Aug	**Sept**	**Aug**	**Sept**	**Aug**	**Sept**	**Aug**	**Sept**	**Aug**	**Sept**
Community uptake (nmol L^{-1} h^{-1})	82 ± 7	68 ± 6	17 ± 6	22 ± 2	67 ± 7	38 ± 3	35 ± 2	5 ± 0	1115	456
Single-cell Pcy uptake (nmol L^{-1} h^{-1})	5 ± 1	23 ± 6	$3 \pm 2 \times 10^{-1}$	1 ± 1	3 ± 1	15 ± 13	1 ± 0	2 ± 0	42 ± 6	163 ± 14
Single-cell Pcy uptake (%)	6	34	2	5	4	40	3	34	4	36
Colony-forming Pcy uptake (nmol L^{-1} h^{-1})	$4 \pm 3 \times 10^{-2}$	—	$0 \pm 0 \times 10^{-2}$	—	$3 \pm 2 \times 10^{-2}$	—	$2 \pm 1 \times 10^{-2}$	—	$5 \pm 3 \times 10^{-1}$	—
Colony-forming Pcy uptake (%)	< 1	—	< 1	—	< 1	—	< 1	—	< 1	—

dissolved organic carbon (Bunse et al. 2019) with the phytoplankton, as assessed by biomass, transitioning from cyanobacteria- to flagellate-dominant communities (Fridolfsson et al. 2023). Meanwhile, picocyanobacteria regularly do not decrease in abundance until November (Alegria Zufia et al. 2022). The seasonal abundances, diversity and biomass contribution of single-cell picocyanobacteria is increasingly recognized (Celepli et al. 2017; Alegria Zufia et al. 2022), while the seasonal dynamics of colony-forming picocyanobacteria are not well described (Albrecht et al. 2017; Celepli et al. 2017). Our central Baltic Sea time-series data showed that colony-formers, including the genera *Anathece*, *Aphanothece*, *Aphanocapsa*, *Cyanodictyon*, and *Woronichinia*, contribute substantially to the total phytoplankton biomass, especially during summer (July–August). The initial annual increase in abundance of colony-formers was similar to that observed for single-cell picocyanobacteria (Alegria Zufia et al. 2022), with accumulation beginning in late June and early July. However, the abundances of colony-formers appear to decline earlier (September) than the single-cell lifestyle. Abundances of colony-formers were highly variable between the years, suggesting sensitive regulation by unknown top-down or bottom-up environmental conditions or other unknown factors. Multiple examples of top-down control on colony-forming species have been observed in Swedish freshwater lake systems, where the reduction of zooplankton or small fish coincides with increases in biomass (Bergman et al. 1999; Cronberg 1999). Meanwhile, some colony-formers (Chroococcales) co-occur with N_2-fixing filamentous cyanobacteria (Hajdu et al. 2007) and may be stimulated by high phosphorus, low N environments (Andersson et al. 2015), revealing a bottom-up influence on growth. There are also multiple studies showing that primary production is partially supported by the transfer of newly fixed N throughout the phytoplankton community, either through release of the fixed N into the dissolved pool or through coupling between nitrifiers and co-occurring picocyanobacteria (Caffin et al. 2018; Klawonn et al. 2019).

In addition to the factors affecting growth and abundance, shifts from colony- to single-cell lifestyles can also occur within the picocyanobacteria community. Komárek et al. (2014) report that environmental conditions may influence colony formation and that cultivated colonies can lose the cohesive mucilaginous envelopes to adopt single-cell lifestyles. Furthermore, *Cyanodictyon*, a member of Synechococcales, can consist of both colony and single-cell populations in natural communities, as well as rapidly form larger colonies in the presence of predators (Huber et al. 2017). Further freshwater *Synechococcus* can be stimulated to form colonies in the presence of nanoflagellate grazers (Callieri et al. 2016). These may have additionally influenced the perceived abundances of colony-forming and single-cell species when observed through microscopy in this study.

Molecular studies investigating Baltic Sea picocyanobacterial abundances and diversity have largely overlooked colony-forming species (Celepli et al. 2017; Bennke et al. 2018; Alegria Zufia et al. 2022). This may partially be due to their genetic similarities to genera largely considered as free-living. The reclassification of many members of *Aphanothece* to *Anathece*, which have been placed in the same clade as *Cyanobium* (Komárek et al. 2011), reveals how close many of these organisms are at the genetic level. Our phylogenetic analysis showed that 16S rRNA gene sequences from *Aphanothece* (*Anathece*) spp. clustered within Synechococcales, with very similar or identical sequences from representative *Cyanobium* and *Synechococcus* strains. It is well known from previous studies that the 16S rRNA gene does not well define *Synechococcus* strains and therefore should be interpreted cautiously. However, this also highlights how the presence and dynamics of *Anathece* could be overlooked and misinterpreted as single-cell taxa when only using the 16S rRNA gene to identify environmental sequences. Furthermore, our microscopy cell counts showed a clear shift in the colony-forming and single-cell abundances between August and September 2020, while changes in community composition were also observed in the amplicon libraries. The relatively abundant ASV_00038 had the greatest change in mean proportion, while several of the less abundant ASVs in August were absent in September. It is possible that these ASVs represent some of the colonial forms present in August but not September. Some of these ASVs were mapped to phyla that

exhibit single-cell (or parasitic in the case for *Vampirovibrio*) lifestyles; however, due to the poor representation of colonial picocyanobacteria in genetic databases, the confidence in these assignments is questionable. Notably, *A. paralleliformis* and *Aphanothece* sp. strains from the Baltic Sea do not currently have genetic representation. Meanwhile, *Anathece* spp. are vastly underrepresented in genetic databases compared to *Cyanobium* and *Synechococcus* (Komárek et al. 2014). Thus, for a clearer understanding of colony-forming picocyanobacterial taxonomy, seasonality, and diversity in the Baltic Sea, future studies focusing on identifying gene regions that successfully delineate functional diversity are necessary, as well as the isolation and sequencing of colony-forming strains.

In the present study, we showed that picocyanobacteria were important contributors to phytoplankton biomass and C and N uptake in August and September 2020. Picocyanobacteria were particularly important to the community uptake in September when they accounted for one third or more of the total C fixation and N uptake, while contributing up to 6% of the uptake in August. These differences may be influenced by the nutrient environment. N availability has previously been observed to influence uptake rates of inorganic and organic N substrates in the Gulf of Riga (Berg et al. 2001). In our study, higher concentrations of NO_3 in September were accompanied by twofold higher NO_3 N-specific uptake. Also, following the seasonal decrease in dissolved organics (Bunse et al. 2019), lower DFAA concentrations in September accompanied lower DFAA uptake rates, which indicates that uptake may have been lower due to the limiting concentrations in the water. However, the inverse dynamic observed for urea and NH_4 suggest internal cellular factors may also influence uptake rates. Both phytoplankton and cyanobacteria can regulate uptake based on N substrates present in the environment. In strains of *Synechococcus*, NO_3 uptake can be suppressed in the presence of NH_4 (Collier et al. 2012). Similarly, urea uptake is regulated by the presence of other N substrates in both phytoplankton and cyanobacteria, though patterns of regulation vary among taxonomic groups (Solomon et al. 2010). Therefore, an interplay in the availability of N substrates and cellular responses may have influenced uptake rates.

In September, picocyanobacteria accounted for > 30% of the C and N uptake. This was primarily due to the single-cell picocyanobacteria. Colony-formers, on the other hand did not contribute highly to C or N uptake during either experiment, generally due to their lower abundances and lower N-specific uptake rates. Similarly, Klawonn et al. (2019) observed lower N-specific NH_4 uptake rates for Baltic Sea colonial compared to single-cell picocyanobacteria. This could be associated with higher nutrient uptake efficiency associated with the smaller size of single cells (Lindemann et al. 2016). In addition, colonial cells may have lower affinity depending on colony characteristics, as colonies that are tightly packed with low surface area have lower exposure to the surrounding environment (Gaedke 1992) while colonies that are porous and loose have greater exposure (Sommer et al. 2001). *A. paralleliformis* forms colonies that are elongated containing hundreds of cells and the colony size, could influence the proximity of these cells to the nutrient environment. It should also be noted that the cell-specific uptake rate calculations for the different groups was based on available C quotas, but this could vary among different strains and growth stage as well as environmental variables such as light and nutrients.

Previous studies have shown that populations within the picophytoplankton differ in C and N uptake rates and have N source preferences (Berthelot et al. 2019). In addition, it was recently shown that populations of Baltic Sea photosynthetic picoeukaryotes and *Synechococcus* respond differently to additions of NO_3 and NH_4 during different seasons (Alegria Zufia et al. 2021). Although, there is a documented preference for NH_4 uptake in *Synechococcus* (Luque et al. 1994; Lindell et al. 1998), strains of *Synechococcus* differ in their uptake rates of NH_4 and NO_3 (Glibert and Ray 1990). The N-specific uptake rates of single cells were significantly higher for NH_4 and urea in September compared to August. This could have been caused by a shift in the composition of picocyanobacteria as indicated by changes in relative abundances of dominating ASVs during our experiments. It is also possible that the presence of N_2-fixing filamentous cyanobacteria in August provided a fraction of the NH_4 being utilized by the picocyanobacteria and reduced the observed uptake with the ^{15}N-labeled substrate.

Our study shows that picocyanobacteria in the central Baltic Sea are significant contributors to the uptake of inorganic C and N as well as organic forms of N during late summer. This underscores the need for including picocyanobacteria, which are often overlooked in monitoring programs, as a functional phytoplankton group. The study also provides novel insights into colonial picocyanobacterial forms which are largely understudied. Our data suggest that single-cell picocyanobacteria provide a much greater contribution to N and C uptake than colony-forming. While colony-forming picocyanobacteria only contributed to a small percentage of the uptake and were relatively rare, their capacity to reach high abundances suggest they may periodically have significant influence on N and C cycling.

Data availability statement

The amplicon sequencing data has been submitted to SRA with the accession number PRJNA841351.

References

Aguilera, A., and others. 2023. Ecophysiological analysis reveals distinct environmental preferences in closely related Baltic Sea picocyanobacteria. Environ. Microbiol. **25**: 1674–1695. doi:10.1111/1462-2920.16384

Albrecht, M., T. Pröschold, and R. Schumann. 2017. Identification of cyanobacteria in a eutrophic coastal lagoon on the Southern Baltic Coast. Front. Microbiol. **8**: 923.

Alegria Zufia, J., H. Farnelid, and C. Legrand. 2021. Seasonality of coastal picophytoplankton growth, nutrient limitation, and biomass contribution. Front. Microbiol. **12**: 786590. doi:10.3389/fmicb.2021.786590

Alegria Zufia, J., C. Legrand, and H. Farnelid. 2022. Seasonal dynamics in picocyanobacterial abundance and clade composition at coastal and offshore stations in the Baltic Sea. Sci. Rep. **12**: 14330.

Andersson, A., H. Höglander, C. Karlsson, and S. Huseby. 2015. Key role of phosphorus and nitrogen in regulating cyanobacterial community composition in the northern Baltic Sea. Estuar. Coast. Shelf Sci. **164**: 161–171. doi:10.1016/j.ecss.2015.07.013

Baer, S. E., M. W. Lomas, K. X. Terpis, C. Mouginot, and A. C. Martiny. 2017. Stoichiometry of *Prochlorococcus*, *Synechococcus*, and small eukaryotic populations in the western North Atlantic Ocean. Environ. Microbiol. **19**: 1568–1583. doi:10.1111/1462-2920.13672

Barbera, P., A. M. Kozlov, L. Czech, B. Morel, D. Darriba, T. Flouri, and A. Stamatakis. 2018. EPA-ng: Massively parallel evolutionary placement of genetic sequences. Syst. Biol. **68**: 365–369.

Bennke, C., F. Pollehne, A. Müller, R. Hansen, B. Kreikemeyer, and M. Labrenz. 2018. The distribution of phytoplankton in the Baltic Sea assessed by a prokaryotic 16S rRNA gene primer system. J. Plankton Res. **40**: 244–254. doi:10.1093/plankt/fby008

Berg, G. M., P. M. Glibert, N. O. Jørgensen, M. Balode, and I. Purina. 2001. Variability in inorganic and organic nitrogen uptake associated with riverine nutrient input in the Gulf of Riga, Baltic Sea. Estuaries **24**: 204–214. doi:10.2307/1352945

Berg, G. M., M. Balode, I. Purina, S. Bekere, C. Béchemin, and S. Y. Maestrini. 2003. Plankton community composition in relation to availability and uptake of oxidized and reduced nitrogen. Aquat. Microb. Ecol. **30**: 263–274. doi:10.3354/ame030263

Bergman, E., S. F. Hamrin, and P. Romare. 1999. The effects of cyprinid reduction on the fish community, p. 65–75. *In* L.-A. Hansson, and E. Bergman [eds.], Nutrient reduction and biomanipulation as tools to improve water quality: The Lake Ringsjön story. Springer.

Berthelot, H., S. Duhamel, S. L'Helguen, J.-F. Maguer, S. Wang, I. Cetinić, and N. Cassar. 2019. NanoSIMS single cell analyses reveal the contrasting nitrogen sources for small phytoplankton. ISME J. **13**: 651–662. doi:10.1038/s41396-018-0285-8

Berthelot, H., S. Duhamel, S. L'Helguen, J.-F. Maguer, and N. Cassar. 2021. Inorganic and organic carbon and nitrogen uptake strategies of picoplankton groups in the northwestern Atlantic Ocean. Limnol. Oeanogr. **66**: 3682–3696.

Bokulich, N. A., and others. 2018. Optimizing taxonomic classification of marker-gene amplicon sequences with QIIME 2's q2-feature-classifier plugin. Microbiome **6**: 1–17. doi:10.1186/s40168-018-0470-z

Bolyen, E., and others. 2019. Reproducible, interactive, scalable and extensible microbiome data science using QIIME 2. Nat. Biotech. **37**: 852–857.

Bunse, C., and others. 2019. High frequency multi-year variability in Baltic Sea microbial plankton stocks and activities. Front. Microbiol. **9**: 3296.

Cabello-Yeves, P. J., A. Picazo, A. Camacho, C. Callieri, R. Rosselli, J. J. Roda-Garcia, F. H. Coutinho, and F. Rodriguez-Valera. 2018. Ecological and genomic features of two widespread freshwater picocyanobacteria. Environ. Microbiol. **20**: 3757–3771. doi:10.1111/1462-2920.14377

Cabello-Yeves, P. J., and others. 2022. Elucidating the picocyanobacteria salinity divide through ecogenomics of new freshwater isolates. BMC Biol. **20**: 1–24.

Caffin, M., H. Berthelot, V. Cornet-Barthaux, A. Barani, and S. Bonnet. 2018. Transfer of diazotroph-derived nitrogen to the planktonic food web across gradients of N_2 fixation activity and diversity in the western tropical South Pacific Ocean. Biogeosciences **15**: 3795–3810. doi:10.5194/bg-15-3795-2018

Callahan, B. J., P. J. McMurdie, M. J. Rosen, A. W. Han, A. J. A. Johnson, and S. P. Holmes. 2016. DADA2: High-resolution sample inference from Illumina amplicon data. Nat. Methods **13**: 581–583. doi:10.1038/nmeth.3869

Callieri, C. 2008. Picophytoplankton in freshwater ecosystems: The importance of small-sized phototrophs. Freshw. Rev. **1**: 1–28. doi:10.1608/FRJ-1.1.1

Callieri, C. 2010. Single cells and microcolonies of freshwater picocyanobacteria: A common ecology. J. Limnol. **69**: 257–277. doi:10.4081/jlimnol.2010.257

Callieri, C., A. Lami, and R. Bertoni. 2011. Microcolony formation by single-cell *Synechococcus* strains as a fast response to UV radiation. Appl. Environ. Microbiol. **77**: 7533–7540. doi:10.1128/AEM.05392-11

Callieri, C., G. Cronberg, and J. G. Stockner. 2012. Freshwater picocyanobacteria: Single cells, microcolonies and colonial forms, p. 229–269. *In* Ecology of cyanobacteria II. Springer.

Callieri, C., S. Amalfitano, G. Corno, and R. Bertoni. 2016. Grazing-induced *Synechococcus* microcolony formation: Experimental insights from two freshwater phylotypes. FEMS Microbiol. Ecol. **92**: fiw154. doi:10.1093/femsec/fiw154

Capella-Gutiérrez, S., J. M. Silla-Martínez, and T. Gabaldón. 2009. trimAl: A tool for automated alignment trimming in large-scale phylogenetic analyses. Bioinformatics **25**: 1972–1973. doi:10.1093/bioinformatics/btp348

Celepli, N., J. Sundh, M. Ekman, C. L. Dupont, S. Yooseph, B. Bergman, and K. Ininbergs. 2017. Meta-omic analyses of Baltic Sea cyanobacteria: Diversity, community structure and salt acclimation. Environ. Microbiol. **19**: 673–686. doi:10.1111/1462-2920.13592

Collier, J. L., R. Lovindeer, Y. Xi, J. C. Radway, and R. A. Armstrong. 2012. Differences in growth and physiology of marine *Synechococcus* (cyanobacteria) on nitrate versus ammonium are not determined solely by nitrogen source redox state. J. Phycol. **48**: 106–116. doi:10.1111/j.1529-8817.2011.01100.x

Cronberg, G. 1999. Qualitative and quantitative investigations of phytoplankton in Lake Ringsjön, Scania, Sweden, p. 27–40. *In* Nutrient reduction and biomanipulation as tools to improve water quality: The Lake Ringsjön story. Springer.

Czech, L., P. Barbera, and A. Stamatakis. 2020. Genesis and Gappa: Processing, analyzing and visualizing phylogenetic (placement) data. Bioinformatics **36**: 3263–3265. doi:10.1093/bioinformatics/btaa070

Farrant, G. K., and others. 2016. Delineating ecologically significant taxonomic units from global patterns of marine picocyanobacteria. Proc. Natl. Acad. Sci. USA **113**: E3365–E3374. doi:10.1073/pnas.1524865113

Flombaum, P., and others. 2013. Present and future global distributions of the marine cyanobacteria *Prochlorococcus* and *Synechococcus*. Proc. Natl. Acad. Sci. USA **110**: 9824–9829. doi:10.1073/pnas.1307701110

Fridolfsson, E., C. Bunse, E. Lindehoff, H. Farnelid, B. Pontiller, K. Bergström, J. Pinhassi, C. Legrand, and S. Hylander. 2023. Multiyear analysis uncovers coordinated seasonality in stocks and composition of the planktonic food web in the Baltic Sea proper. Sci. Rep. **13**: 11865.

Fuller, N. J., D. Marie, F. Partensky, D. Vaulot, A. F. Post, and D. J. Scanlan. 2003. Clade-specific 16S ribosomal DNA oligonucleotides reveal the predominance of a single marine *Synechococcus* clade throughout a stratified water column in the Red Sea. Appl. Environ. Microbiol. **69**: 2430–2443. doi:10.1128/AEM.69.5.2430-2443.2003

Gaedke, U. 1992. The size distribution of plankton biomass in a large lake and its seasonal variability. Limnol. Oceanogr. **37**: 1202–1220. doi:10.4319/lo.1992.37.6.1202

Glibert, P., and R. Ray. 1990. Different patterns of growth and nitrogen uptake in two clones of marine *Synechococcus* spp. Mar. Biol. **107**: 273–280. doi:10.1007/BF01319826

Grasshoff, K., K. Kremling, and M. Ehrhardt. 2009. Methods of seawater analysis. Wiley.

Hagström, Å., U. L. Zweifel, J. Sundh, C. M. G. Osbeck, C. Bunse, J. Sjösted, B. Müller-Karulis, and J. Pinhassi. 2021. Composition and seasonality of membrane transporters in marine picoplankton. Front. Microbiol. **12**: 2693.

Hajdu, S., H. Höglander, and U. Larsson. 2007. Phytoplankton vertical distributions and composition in Baltic Sea cyanobacterial blooms. Harmful Algae **6**: 189–205. doi:10.1016/j.hal.2006.07.006

HELCOM. 2021. Guidelines for monitoring of phytoplankton species composition, abundance and biomass. HELCOM, p. 22.

Herlemann, D. P., M. Labrenz, K. Jürgens, S. Bertilsson, J. J. Waniek, and A. F. Andersson. 2011. Transitions in bacterial communities along the 2000 km salinity gradient of the Baltic Sea. ISME J. **5**: 1571–1579. doi:10.1038/ismej.2011.41

Hoang, D. T., O. Chernomor, A. von Haeseler, B. Q. Minh, and L. S. Vinh. 2017. UFBoot2: Improving the ultrafast bootstrap approximation. Mol. Biol. Evol. **35**: 518–522.

Huber, P., and others. 2017. Phenotypic plasticity in freshwater picocyanobacteria. Environ. Microbiol. **19**: 1120–1133. doi:10.1111/1462-2920.13638

Jespersen, A.-M., and K. Christoffersen. 1987. Measurements of chlorophyll-a from phytoplankton using ethanol as extraction solvent. Arch. Hydrobiol. **109**: 445–454. doi:10.1127/archiv-hydrobiol/109/1987/445

Jezberová, J., and J. Komárková. 2007. Morphological transformation in a freshwater *Cyanobium* sp. induced by grazers. Environ. Microbiol. **9**: 1858–1862. doi:10.1111/j.1462-2920.2007.01311.x

Kalyaanamoorthy, S., B. Q. Minh, T. K. F. Wong, A. von Haeseler, and L. S. Jermiin. 2017. ModelFinder: Fast model selection for accurate phylogenetic estimates. Nat. Methods **14**: 587–589. doi:10.1038/nmeth.4285

Klawonn, I., S. Bonaglia, M. J. Whitehouse, S. Littmann, D. Tienken, M. M. M. Kuypers, V. Brüchert, and H. Ploug. 2019. Untangling hidden nutrient dynamics: Rapid ammonium cycling and single-cell ammonium assimilation in marine plankton communities. ISME J. **13**: 1960–1974. doi:10.1038/s41396-019-0386-z

Komárek, J., J. Kaštovský, and J. Jezberová. 2011. Phylogenetic and taxonomic delimitation of the cyanobacterial genus *Aphanothece* and description of *Anathece* gen. nov. Eur. J. Phycol. **46**: 315–326. doi:10.1080/09670262.2011.606373

Komárek, J., J. Kaštovský, J. Mareš, and J. R. Johansen. 2014. Taxonomic classification of cyanoprokaryotes (cyanobacterial genera) 2014, using a polyphasic approach. Preslia **86**: 295–335.

Komárková, J., and K. Šimek. 2003. Unicellular and colonial formations of picoplanktonic cyanobacteria under variable environmental conditions and predation pressure. Algol. Stud. Arch. Hydrobiol. **109**: 327–340.

Laamanen, M. J. 1997. Environmental factors affecting the occurrence of different morphological forms of cyanoprokaryotes in the northern Baltic Sea. J. Plankton Res. **19**: 1385–1403. doi:10.1093/plankt/19.10.1385

Legrand, C., E. Fridolfsson, M. Bertos-Fortis, E. Lindehoff, P. Larsson, J. Pinhassi, and A. Andersson. 2015. Interannual variability of phyto-bacterioplankton biomass and production in coastal and offshore waters of the Baltic Sea. Ambio **44**: 427–438. doi:10.1007/s13280-015-0662-8

Letunic, I., and P. Bork. 2019. Interactive tree of life (iTOL) v4: Recent updates and new developments. Nucleic Acids Res. **47**: W256–W259. doi:10.1093/nar/gkz239

Lindell, D., E. Padan, and A. F. Post. 1998. Regulation of *ntcA* expression and nitrite uptake in the marine *Synechococcus* sp. strain WH 7803. J. Bacteriol. **180**: 1878–1886. doi:10.1128/JB.180.7.1878-1886.1998

Lindemann, C., Ø. Fiksen, K. H. Andersen, and D. L. Aksnes. 2016. Scaling laws in phytoplankton nutrient uptake affinity. Front. Mar. Sci. **3**: 26.

Luque, I., E. Flores, and A. Herrero. 1994. Molecular mechanism for the operation of nitrogen control in cyanobacteria. EMBO J. **13**: 2862–2869. doi:10.1002/j.1460-2075.1994.tb06580.x

Łysiak-Pastuszak, E., and others. 2012. A study of episodic events in the Baltic Sea-combined in situ and satellite observations. Oceanologia **54**: 121–141. doi:10.5697/oc.54-2.121

MacKeigan, P. W., and others. 2022. Comparing microscopy and DNA metabarcoding techniques for identifying cyanobacteria assemblages across hundreds of lakes. Harmful Algae **113**: 102187. doi:10.1016/j.hal.2022.102187

Mattsson, L., and others. 2021. Functional diversity facilitates stability under environmental changes in an outdoor microalgal cultivation system. Front. Bioeng. Biotechnol. **9**: 651895. doi:10.3389/fbioe.2021.651895

Maugeri, T. L., V. Lentini, A. Spanò, and C. Gugliandolo. 2013. Abundance and diversity of picocyanobacteria in shallow hydrothermal vents of Panarea Island (Italy). Geomicrobiol. J. **30**: 93–99. doi:10.1080/01490451.2011.653088

Michelou, V. K., M. T. Cottrell, and D. L. Kirchman. 2007. Light-stimulated bacterial production and amino acid assimilation by cyanobacteria and other microbes in the North Atlantic Ocean. Appl. Environ. Microbiol. **73**: 5539–5546. doi:10.1128/AEM.00212-07

Moore, L. R., A. F. Post, G. Rocap, and S. W. Chisholm. 2002. Utilization of different nitrogen sources by the marine cyanobacteria *Prochlorococcus* and *Synechococcus*. Limnol. Oceanogr. **47**: 989–996. doi:10.4319/lo.2002.47.4.0989

Mulvenna, P. F., and G. Savidge. 1992. A modified manual method for the determination of urea in seawater using diacetylmonoxime reagent. Estuar. Coast. Shelf Sci. **34**: 429–438. doi:10.1016/S0272-7714(05)80115-5

Muñoz-Marín, M., G. Gómez-Baena, A. López-Lozano, J. Moreno-Cabezuelo, J. Díez, and J. García-Fernández. 2020. Mixotrophy in marine picocyanobacteria: Use of organic compounds by *Prochlorococcus* and *Synechococcus*. ISME J. **14**: 1065–1073. doi:10.1038/s41396-020-0603-9

Nguyen, L.-T., H. A. Schmidt, A. von Haeseler, and B. Q. Minh. 2014. IQ-TREE: A fast and effective stochastic algorithm for estimating maximum-likelihood phylogenies. Mol. Biol. Evol. **32**: 268–274.

Olson, R., S. Chisholm, E. Zettler, and E. Armbrust. 1988. Analysis of *Synechococcus* pigment types in the sea using single and dual beam flow cytometry. Deep Sea Res. A Oceanogr. Res. Pap. **35**: 425–440. doi:10.1016/0198-0149(88)90019-2

Parsons, T. R., Y. Maita, and C. M. Lalli. 1984. A manual of chemical and biological methods for seawater analysis, 1st ed. Pergamon Press.

Redfield, A. C. 1958. The biological control of chemical factors in the environment. Am. Sci. **46**: 205–221.

Rutten, T. P., B. Sandee, and A. R. Hofman. 2005. Phytoplankton monitoring by high performance flow cytometry: A successful approach? Cytom. J. Int. Soc. Anal. Cytol. **64**: 16–26.

Salcher, M. M., T. Posch, and J. Pernthaler. 2013. In situ substrate preferences of abundant bacterioplankton populations in a prealpine freshwater lake. ISME J. **7**: 896–907. doi:10.1038/ismej.2012.162

Schneider, C. A., W. S. Rasband, and K. W. Eliceiri. 2012. NIH image to ImageJ: 25 years of image analysis. Nat. Methods **9**: 671–675. doi:10.1038/nmeth.2089

Solomon, C. M., J. L. Collier, G. M. Berg, and P. M. Glibert. 2010. Role of urea in microbial metabolism in aquatic systems: A biochemical and molecular review. Aquat. Microb. Ecol. **59**: 67–88. doi:10.3354/ame01390

Sommer, U., F. Sommer, B. Santer, C. Jamieson, M. Boersma, C. Becker, and T. Hansen. 2001. Complementary impact of copepods and cladocerans on phytoplankton. Ecol. Lett. **4**: 545–550. doi:10.1046/j.1461-0248.2001.00263.x

Somogyi, B., T. Felföldi, L. G. Tóth, G. Bernát, and L. Vörös. 2020. Photoautotrophic picoplankton–a review on their occurrence, role and diversity in Lake Balaton. Biol. Futura **71**: 371–382. doi:10.1007/s42977-020-00030-8

Stal, L. J., P. Albertano, B. Bergman, H. von Bröckel, J. R. Gallon, P. K. Hayes, K. Sivonen, and A. E. Walsby. 2003. BASIC: Baltic Sea cyanobacteria. An investigation of the structure and dynamics of water blooms of cyanobacteria in the Baltic Sea—Responses to a changing environment. Cont. Shelf Res. **23**: 1695–1714. doi:10.1016/j.csr.2003.06.001

Straub, D., N. Blackwell, A. Langarica-Fuentes, A. Peltzer, S. Nahnsen, and S. Kleindienst. 2020. Interpretations of environmental microbial community studies are biased by the selected 16S rRNA (gene) amplicon sequencing pipeline. Front. Microbiol. **11**: 2652. doi:10.3389/fmicb.2020.550420

Utermöhl, H. 1958. Zur vervollkommnung der quantitativen phytoplankton-methodik: Mit 1 Tabelle und 15 abbildungen im Text und auf 1 Tafel. Int. Verein. Theor. Angew. Limnol. Mitt. **9**: 1–38.

Valderrama, J. 1995, p. 262–265. *In* G. M. Hallegraeff, D. M. Anderson, and A. D. Cembella [eds.], Manual on harmful marine microalgae. IOC manuals and guides.

Xiao, M., M. Li, and C. S. Reynolds. 2018. Colony formation in the cyanobacterium Microcystis. Biol. Rev. **93**: 1399–1420. doi:10.1111/brv.12401

Acknowledgments

Conflict of Interest

None declared.